

# Caveolin-1 is required for lateral line neuromast and notochord development

Susan J. Nixon<sup>1,2,3</sup>, Adrian Carter<sup>3</sup>, Jeremy Wegner<sup>4</sup>, Charles Ferguson<sup>1,2,3</sup>, Matthias Floetenmeyer<sup>1,2,3</sup>, Jamie Riches<sup>2</sup>, Brian Key<sup>3</sup>, Monte Westerfield<sup>4</sup> and Robert G. Parton<sup>1,2,3,\*</sup>

<sup>1</sup>Institute for Molecular Bioscience, <sup>2</sup>Centre for Microscopy and Microanalysis and <sup>3</sup>School of Biomedical Sciences, University of Queensland, Brisbane 4072, Australia

<sup>4</sup>Institute of Neuroscience, University of Oregon, Eugene, OR 97403, USA

\*Author for correspondence (e-mail: r.parton@imb.uq.edu.au)

Accepted 23 April 2007

Journal of Cell Science 120, 2151–2161 Published by The Company of Biologists 2007

doi:10.1242/jcs.003830

## Summary

Caveolae have been linked to diverse cellular functions and to many disease states. In this study we have used zebrafish to examine the role of caveolin-1 and caveolae during early embryonic development. During development, expression is apparent in a number of tissues including Kupffer's vesicle, tailbud, intersomite boundaries, heart, branchial arches, pronephric ducts and periderm. Particularly strong expression is observed in the sensory organs of the lateral line, the neuromasts and in the notochord where it overlaps with expression of caveolin-3. Morpholino-mediated downregulation of Cav1 $\alpha$  caused a dramatic inhibition of neuromast formation. Detailed ultrastructural analysis, including electron tomography of the notochord, revealed

that the central regions of the notochord has the highest density of caveolae of any embryonic tissue comparable to the highest density observed in any vertebrate tissue. In addition, Cav1 $\alpha$  downregulation caused disruption of the notochord, an effect that was enhanced further by Cav3 knockdown. These results indicate an essential role for caveolin and caveolae in this vital structural and signalling component of the embryo.

Supplementary material available online at

<http://jcs.biologists.org/cgi/content/full/120/13/2151/DC1>

Key words: Caveolae, Caveolin-1, Neuromast, Notochord, Zebrafish

## Introduction

Caveolae are specialised plasma membrane microdomains enriched in glycosphingolipids, cholesterol and integral membrane proteins termed caveolins. These small 50–80 nm 'cave-like' invaginations of the plasma membrane are found in many cell types but are particularly abundant in adipocytes, endothelial cells and muscle cells (Parton and Simons, 2007; Rothberg et al., 1992; Scherer et al., 1996; Tang et al., 1996; Way and Parton, 1995). Determining the role of caveolins and caveolae in normal tissues is fundamental to understanding their role in diseases such as cancer, where caveolin is a candidate tumour suppressor gene and in muscle disease, where mutations in caveolin have been associated with a number of different clinical symptoms and conditions (Li et al., 2006; Razani and Lisanti, 2001; Williams and Lisanti, 2005). Caveolins are a family of small integral membrane proteins that bind cholesterol and fatty acids (Murata et al., 1995; Trigatti et al., 1999). Three caveolin genes exist in higher eukaryotic genomes. Caveolin-1 (*Cav1*) and Caveolin-2 (*Cav2*) are expressed in numerous tissues in mammalian cells with particularly high expression in tissues with abundant caveolae, whereas caveolin-3 (*Cav3*) is the major caveolin isoform in skeletal and cardiac muscle (Tang et al., 1996; Way and Parton, 1995). The *Cav1* and *Cav2* genes each generate two isoforms. In the case of *Cav1*, alternative transcription initiation sites produce two separate mRNA species (Kogo and Fujimoto, 2000).

*Cav1* has been implicated in an increasing number of cellular processes by the study of *Cav1*-null mice and by downregulation of *Cav1* expression in cultured cells. *Cav1* is

sufficient to drive the formation of caveolae in lymphocytes, which do not normally express caveolins (Fra et al., 1995), and ablation of *Cav1* in mice results in a lack of caveolae in all cells where *Cav1* is normally expressed (Drab et al., 2001; Parton, 2001; Razani et al., 2001). Although *Cav1*-null mice are relatively healthy and fertile with a relatively mild phenotype, in-depth characterisation of these mice has revealed a wide range of effects (Drab et al., 2001; Razani et al., 2001). These studies implicate caveolae in a broad range of cellular activities including lipid regulation, cell signalling and mechanosensation (Parton and Simons, 2007). For example, *Cav1*-null mice show resistance to diet-induced obesity indicating changes in lipid metabolism or adipocyte function (Drab et al., 2001; Razani et al., 2002), consistent with *in vitro* studies (Cohen et al., 2004; Frank et al., 2001; Le Lay et al., 2001). Loss of *Cav1* also leads to reduced survival of mice after partial hepatectomy (Fernandez et al., 2006) associated with a severe reduction in lipid droplet formation and a block in the cell cycle, suggesting an important role for *Cav1* in the co-ordination of lipid metabolism with cell cycle progression (Fernandez et al., 2006). *Cav1*-null mice also show increased sensitivity to carcinogens (Capozza et al., 2003) and changes in mammary development (Williams et al., 2006), consistent with decreased expression of *Cav1* in some tumours (Williams and Lisanti, 2005) and a role for *Cav1* in regulating specific signalling pathways. *Cav1* has also been strongly linked to mechanosensation (Boyd et al., 2003; Parton and Simons, 2007; Radcliff and Rizzo, 2005), particularly in smooth muscle cells (Sedding et al., 2005) and endothelia (Rizzo et al., 2003; Yu et al., 2006). Recent studies have shown a crucial role for

caveolae in linking shear stress generated by laminar flow on the surface of the endothelium to NO generation (Yu et al., 2006).

Despite these numerous studies, a universal role for caveolae linking these apparently diverse functions, which presumably require the unique and conserved architecture of caveolae, is still lacking. We and others have thus started to investigate the function of caveolins in a wider range of eukaryotic systems including the nematode, *Caenorhabditis elegans*, the frog, *Xenopus laevis* and the zebrafish, *Danio rerio*. The *C. elegans* genome contains two caveolin family members (Tang et al., 1997). Cav1 is expressed in most (or all) cells throughout embryonic and larval development. Interference with Cav1 specifically advances meiotic progression in the worm, a process that is Ras/MAP kinase dependent (Scheel et al., 1999). Interestingly, morphological caveolae have not been described in *C. elegans* and recent studies suggest that *C. elegans* caveolin may not generate caveolae (Sato et al., 2006) (M. Kirkham, S.N., D. Wakeham et al., unpublished results).

Here we used zebrafish to study the role of caveolae. Previous Cav1 zebrafish knockdown experiments showed early developmental abnormalities with defects in axis elongation and somite patterning. In these studies, embryos did not survive to 5 days post fertilisation (Fang et al., 2006; Smart et al., 2004). We examined the expression of Cav1 at the mRNA and protein level and the formation of caveolae in various tissues at the ultrastructural level. We also carried out detailed characterisation of Cav1 $\alpha$  function. We show high levels of *cav1* expression in neuromasts of the lateral line, the organs that aid in sensing water movement (Dijkgraaff, 1989). Knockdown of Cav1 $\alpha$  expression disrupts neuromast maturation. We also observe strong expression in the notochord and an incredibly high density of caveolae within specific regions of notochord cells, particularly the cell-cell junctional regions within the centre of the notochord. We also demonstrate the evolutionary conservation of caveolin notochord expression in chick and mouse. We propose a novel structural role for caveolae in the notochord and a hitherto unexpected role in neuromast development.

## Results

### Putative signalling tissues express Cav1 during early development

To further our understanding of Cav1 and its role in development we examined the developmental expression pattern of *cav1* by mRNA in situ hybridisation. *cav1* mRNA first appears in a spatially restricted pattern in the notochord just prior to the six-somite stage (12 hours), and this expression persists throughout most of the segmentation period (Fig. 1A,E). At the six-somite stage, the periderm, a tightly sealed epithelial monolayer of specialised impermeable cells that covers the entire embryo after gastrula stages (Kimmel et al., 1995), also expresses *cav1* (Fig. 1A). Peridermal labelling persists throughout subsequent embryonic and early larval stages (Fig. 1A-G,I-L,N). Later, the epithelial lining (demonstrated by the ring, Fig. 1B) of Kupffer's vesicle (KV) expresses *cav1*. The KV is thought to be important in many signalling processes (Cooper and D'Amico, 1996; Melby et al., 1996). At the 14-20-somite stage (16-19 hours), KV labelling disappears (consistent with loss of this structure) and *cav1* expression is then detected in a cluster of cells in the tailbud,

probably originating from the KV (Fig. 1C,D). The expression in the tailbud persists until the 20-somite stage (Fig. 1E). Thus, during early development, major signalling centres express *cav1*.

By the long-pec stage (48 hours), anterior and posterior lateral line neuromasts express high levels of *cav1* (Fig. 1N; example of labelling at 72 hours). The neuromasts are deposited along the lateral line at regular intervals, from a migrating primordium; however, *cav1* expression is undetectable in the migrating primordium (Fig. 1F). This migration is completed by about 42 hours when the last neuromast is deposited, and neuromasts mature approximately 6 hours later (Gompel et al., 2001), suggesting an association of Cav1 with maturing neuromasts.

At the protruding-mouth stage (72 hours), we observe *cav1* labelling in the heart, branchial arches, gut, pronephric ducts and the intersomite boundaries, presumably representing expression by the vasculature (Fig. 1H-N). By 6 days, *cav1* expression in the heart is restricted to the ventricle (Fig. 1M). The correlation of this mRNA expression pattern with protein levels was confirmed by labelling with a pan-caveolin antibody as used previously (Nixon et al., 2005) (see Fig. 4G,H and Fig. 6A for an example), and a commercially available caveolin antibody seen in sections Fig. 2F and ultrastructurally Fig. 3D.

### Notochord cells develop a high density of intermediate-filament-associated caveolae

The small size of the zebrafish embryo provides the opportunity to analyse the formation of caveolae in various tissues during development and to therefore gain new insights into the role of these structures at specific developmental stages. We analysed the formation of caveolae in tissues that express Cav1 by examining ultrathin sections cut transversely across the zebrafish trunk at various stages of development. We detected a low density of caveolae on the basolateral surface of peridermal cells from 48 hours, consistent with the strong expression of Cav1 in the peridermal layer.

The most dramatic concentration of caveolae forms in the large vacuolating cells of the notochord consistent with caveolin expression (Fig. 2F). After segmentation stages (24 hours), caveolae are present in all cells of the notochord. However, the highest concentration of caveolae is located within the cell-cell junctional regions that cross the centre of the notochord (Fig. 2A-E). This is even more dramatic by 48 hours (Fig. 2B,C,E) and 72 hours; even though the cells are extremely vacuolated and the cytosol largely devoid of other recognisable structures, the central cell-cell contact regions (forming 'struts') across the centre of the notochord show an incredible density of caveolae, greater than the highest density of caveolae observed in any tissue to our knowledge (estimated as 37 caveolae/ $\mu\text{m}^2$  in mouse adipocytes; 38 caveolae/ $\mu\text{m}^2$  in 30-hour notochord; 88 caveolae/ $\mu\text{m}^2$  in 48-hour notochord; see Materials and Methods for details).

In addition to the incredible density of caveolae in the junctional regions of the notochord, we noted a striking organisation of filaments in areas enriched in caveolae. The filaments are largely excluded from the areas enriched in caveolae (Fig. 3A,c) but form a distinct filamentous network to the cytoplasmic side of the caveolae (Fig. 3A,f). To identify these filaments we measured their diameters as  $10\pm 2$  nm. This size corresponds to the size of intermediate filaments.

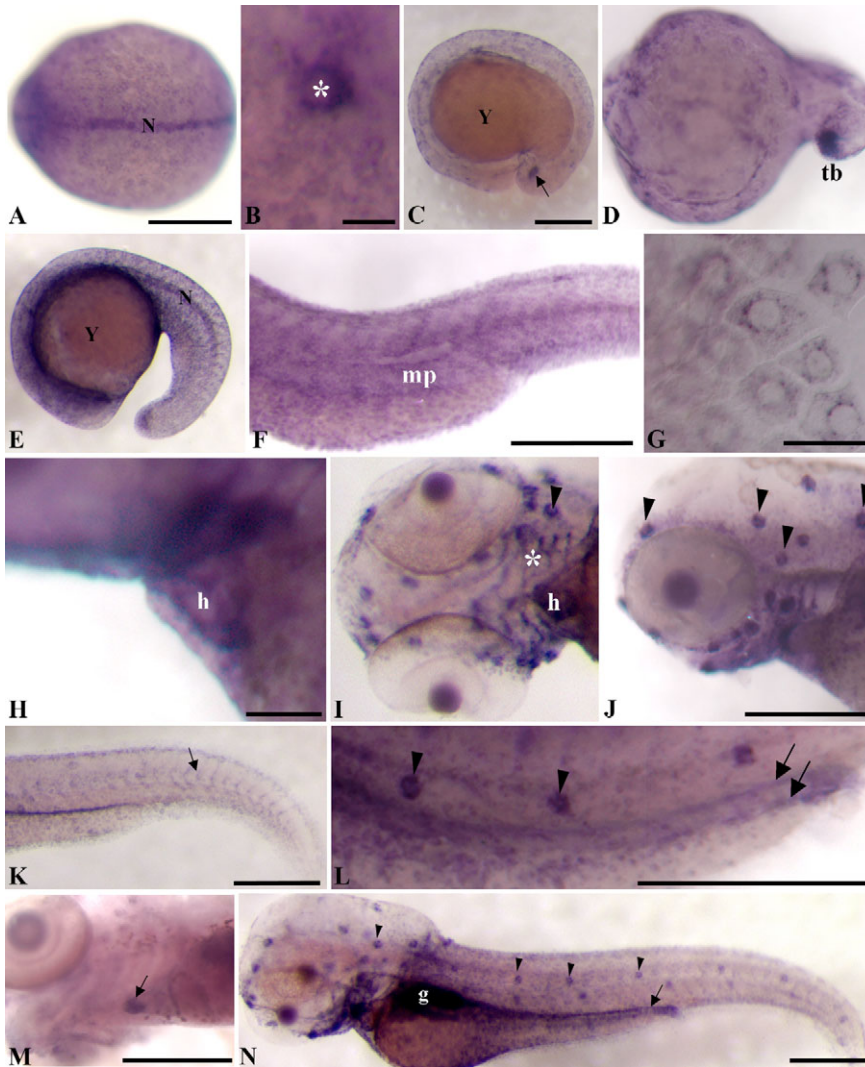
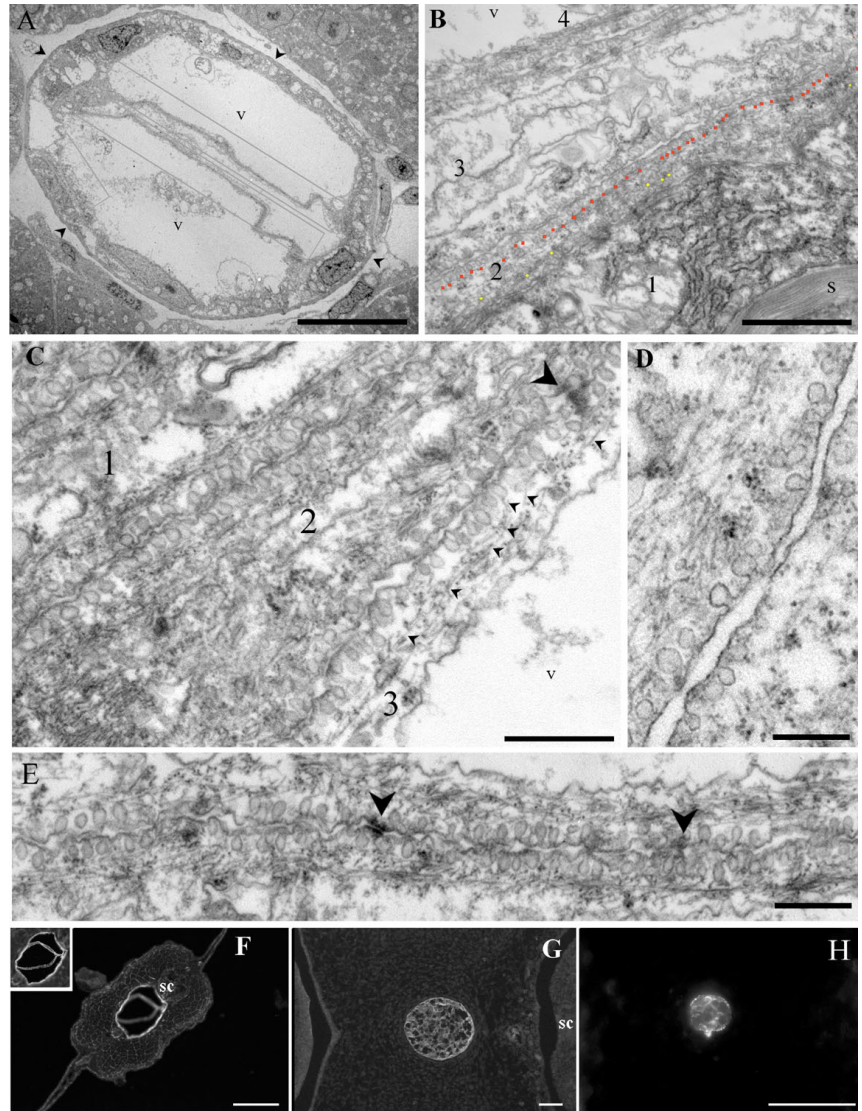


**Fig. 1.** *cav1* localises to key signalling tissues in the developing zebrafish. Developmental expression pattern of *cav1* was analysed by whole-mount mRNA in situ hybridisation. Anterior is to the left and dorsal to the top unless otherwise stated. (A) Dorsal view of a 12-hour embryo where *cav1* expression is detected in the notochord (N). (B) At the same time *cav1* expression can be seen in the epithelial lining of Kupffer's vesicle (posterior view; asterisk). (C-E) Between 16-19 hours *cav1* expression is very high in a cluster of cells within the tailbud (tb) (C, 16 hours, arrow; D, 17 hours), notochord and epidermis. (F) At 36 hours, *cav1* expression is high in the periderm but excluded from the migrating primordium of the lateral line (mp). (G) A magnified view of the periderm at 36 hours shows expression around the nuclei. By 72 hours, expression is apparent in the neuromasts (arrowheads, I, J, L, N), the heart (h, H) the branchial arches (ventral view, asterisk, I) and in the pronephric ducts (arrows, L). (K) At 48 hours expression can be seen in a region near the intersomite borders, probably the intersegmental vessels (arrow). (M) By 6 days, *cav1* expression in the heart is restricted to the ventricle (arrow). Bars, 250  $\mu\text{m}$  (A, also for D and E) (C, F, J-N); 25  $\mu\text{m}$  (B); 10  $\mu\text{m}$  (G); 50  $\mu\text{m}$  (H).

Labelling with a pan-cytokeratin antibody on sections confirmed labelling within the notochord (Fig. 3D,E) and revealed a pattern within the 'struts' similar to the Cav1 labelling (Fig. 3C). Immunogold labelling of the zebrafish notochord revealed caveolin within caveolae and cytokeratin labelling either side of the caveolae consistent with the intermediate filaments seen in Fig. 3A. By electron microscopy, apparent connections between the band of intermediate filaments and the 'bulb' of the caveolae are frequently observed (Fig. 3A, arrowheads). In addition to the intermediate filaments, putative desmosomes are seen (Fig. 2E, arrowheads). To gain further insight into this organisation in 3D at high resolution, we analysed thick sections of 48-hour embryos by electron tomography and generated a dual-axis-tilt series of a 300 nm section of the notochord region of a 3-day post fertilisation embryo (see Movie 1 in supplementary material and single images in Fig. 3B). Connections between intermediate filaments running parallel to the cell surface and the caveolae but not to the junctions are apparent in the tomograms. This unusual organisation suggests a strong link between caveolae, intermediate filaments, and the cell-cell contacts within the notochord.

**Morpholinos downregulate expression of Cav1 $\alpha$  protein**  
To explore the role of Cav1 $\alpha$  during development we first optimised conditions to knockdown Cav1 expression. One- to two-cell-stage embryos were injected with two independent morpholino antisense oligonucleotides (MO), one targeted to the region flanking the start codon of *cav1 $\alpha$*  (*cav1*-MO1) and a second MO directed to a sequence upstream of the start codon in the 5'UTR (*cav1*-MO2). These MOs should inhibit expression of Cav1 $\alpha$  but not Cav1 $\beta$ . Cav1 expression was examined by labelling with a pan-caveolin antibody (Luetterforst et al., 1999), which we have used previously in zebrafish (Nixon et al., 2005). Caveolin labelling at the junctions between peridermal cells (Fig. 4I) and in intersomite boundaries is lost after MO injection (Fig. 4J), but, importantly, labelling of muscle cells known to express Cav3 (Nixon et al., 2005) persists (Fig. 4J) showing the specificity and efficacy of Cav1 knockdown. We also performed western blot analysis on embryos injected with *cav1*-MO1 and *cav1*-MO2 at 48 hours post injection. A band of ~24 kDa was detected by western blot analysis using a caveolin polyclonal antibody in the control MO-injected embryos but embryos injected with either MO targeted to Cav1 show complete

**Fig. 2.** Zebrafish, chick and mouse notochords express caveolin. (A-E) Ultrastructural analysis of caveolae in the notochord during embryonic development. (A) 30-hour zebrafish embryo showing the notochord at low magnification. Arrowheads indicate the sheath surrounding the notochord cells. The notochord cells contain large vacuoles (v) surrounded by a thin layer of cytoplasm. The three boxed areas show the cell-cell contact regions within the notochord where the highest density of caveolae are found. (B) Peripheral area of the notochord of a 48-hour embryo showing several cell-cell contact regions densely covered in caveolae. Four different cells are indicated (1-4). Caveolae in cell 2 are indicated by dots; red dots indicate caveolae on the plasma membrane oriented towards the centre of the notochord (in contact with cell 3), yellow dots indicate caveolae on the cell surface in contact with cell 4. Note the difference in density on the two surfaces of the cell with more caveolae oriented towards the centre of the notochord away from the sheath (s). (C,E) Central area of 48-hour embryos showing high density of caveolae close to longitudinally running filaments (small arrowheads in C). Three different cells are indicated in C (1-3). Note the putative desmosomes (large arrowheads). (D) 24-hour embryos show a lower density of caveolae. (F,G) Paraffin-embedded sections from zebrafish (72 hours, F; inset shows different focal plane), chicken (Stage 24, G), and mouse (E10.5, H) labelled for caveolin; sc, spinal cord. Caveolin expression is high in the notochord of all three species. Bars, 10  $\mu\text{m}$  (A); 1  $\mu\text{m}$  (B); 500 nm (D,E); 50  $\mu\text{m}$  (F-H).



knockdown of Cav1 expression (Fig. 4K). Coomassie Blue staining of the membrane indicates equal protein loading in each lane.

#### Knockdown of Cav1 $\alpha$ affects development of heart and notochord

We then examined the effects of *cav1*-MO1 and *cav1*-MO2 morpholinos, injected at various concentrations, on embryonic development. The *cav1*-MO1-injected embryos consistently show more-severe defects than the *cav1*-MO2 embryos but, importantly, the two morpholinos cause similar effects, which are summarised in Table 1. Injected embryos are characteristically curved and show notochord defects (Fig. 4B,E,F and see below). *cav1*-MO2 injected embryos also display a shortened body axis and blebbing around the blood island (Fig. 4B). At 72 hours, the embryos injected with *cav1*-MO1 at higher concentrations (3 and 4.5 ng/embryo) exhibit enlarged pericardial sacs and abnormal heart chambers with incorrect heart looping. Embryos injected with this MO at higher concentrations also showed identical effects to those shown (Fang et al., 2006) including retinal pigmented epithelial defects, disruption to neural tissues and disorganised somites (not shown). All embryos injected with a control MO up to 4.5 ng/embryo develop normal morphology including hearts. The *cav1* MO phenotype was dose-dependent; embryos injected with 1.5 ng/embryo of *cav1*-MO1, which only caused a partial ablation of Cav1 $\alpha$

expression measured by western blotting (not shown) were generally normal but had slightly curved tails (not shown). Thus, the phenotype observed with two different MOs, but not a control MO even at higher concentrations, correlates with the level of Cav1 reduction and demonstrates the specificity of the effect. A number of additional control experiments were carried out, firstly the *cav1*-MOs were co-injected with a MO to p53 to suppress non-specific off-target defects through the activation of p53 (Langheinrich et al., 2002) at concentrations from 0.3-3 ng/embryo. The same phenotype was observed (results not shown). In addition, embryos coinjected with the two *cav1* MOs at concentrations that do not cause any defects when injected alone, produced identical phenotypes to those described above, demonstrating the specificity of the MOs and confirming that the effects seen are not due to MO toxicity (results not shown).

To further dissect the role of Cav1, we designed a splice-blocking MO directed to the exon2-intron2 splice junction. The MO caused a reduction, but not loss, of full-length *cav1* mRNA as well as a second, smaller band corresponding to mis-spliced

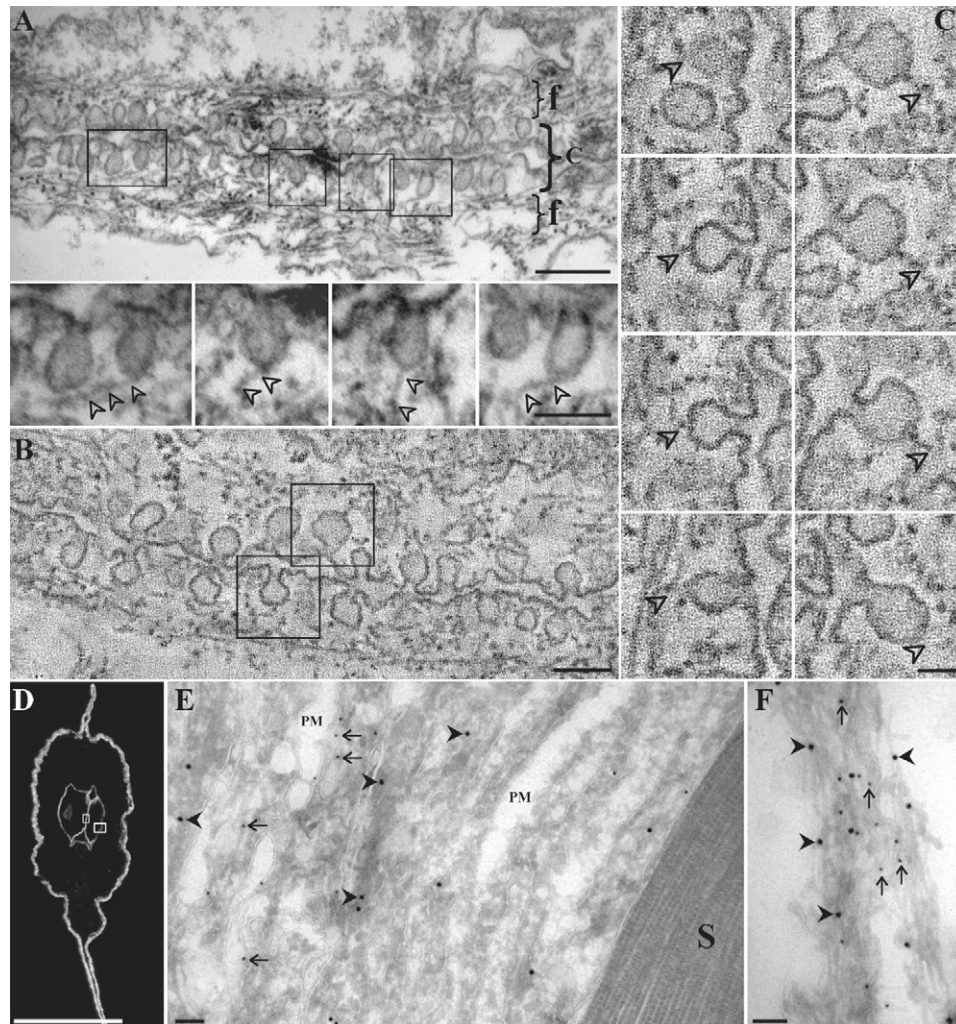


**Fig. 3.** Caveolae interact with intermediate filaments in the notochord. (A) Thin sections of 3-day post fertilisation embryos showing caveolae within the cell-cell contact regions of the notochord. Caveolae (c) at the plasma membrane contact a distinct layer of filaments on the cytoplasmic side (f indicates layer of filaments). Frequent connections (arrowheads) between caveolae and filaments are apparent (boxed areas in A shown in lower panels). (B) Images from a tomogram of the notochord (see supplementary material Movie 1). (C) Images of same areas boxed in B with arrowheads indicating the same areas in different sections. Connections between caveolae and filaments are apparent. (D) Paraffin embedded 72-hour zebrafish sections labelled with a pan-cytokeratin antibody indicating expression in the notochord. Boxed regions demonstrate regions of interest in panel E and F with panel E showing cells in the periphery of the notochord, and panel F showing a central region. (E) In the peripheral regions, caveolin is associated with the plasma membrane between cells (arrows) and keratin is associated with bundles of fibres (arrowhead). (F) In the central strut-like regions of intercellular contact, cytokeratin fibres are found on either side of caveolin-labelled caveolae. Immunogold labelling of 3-day zebrafish sections show caveolin (small gold, arrows) in close proximity to cytokeratin (large gold, arrowheads). Note that the notochord is particularly hard to preserve in frozen sections owing to the large 'empty' vacuoles and extremely thin bridges of cytoplasm in between. S, sheath; PM, plasma membrane. Bars, 200 nm (A,B); 100 nm (inset A,C); 100  $\mu$ m (D); 100 nm (E,F).

RNA as judged by RT-PCR. This is consistent with contribution of maternal mRNA to caveolin expression. We also observed no significant phenotype upon injection of this MO (results not shown). Taken together with the results of Fang et al., this strongly suggests a role of maternally expressed Cav1 at early stages of development (Fang et al., 2006).

#### Caveolin functions in notochord

In view of the incredible abundance of caveolae in the zebrafish notochord, we further examined the effect of Cav1 $\alpha$  MOs on notochord development compared with embryos injected with a control MO. A shortened embryo length is characteristic of

disrupted notochord development (Coutinho et al., 2004; Stemple et al., 1996). Consistent with a role for Cav1 $\alpha$  in the notochord, knockdown of Cav1 $\alpha$  using *cav1*-MO2 causes significantly shorter embryos (Fig. 4L). This was also seen with *cav1*-MO1 but to a lesser extent. At 72 hours, embryos injected with *cav1*-MO2 had a length equivalent to that of control 48-hour embryos ( $3.06 \pm 0.33$  mm,  $n=38$ ; control MO injected embryos  $3.59 \pm 0.18$  mm,  $n=37$ , from three independent experiments). This reduction in length is an underestimate because only straight embryos could be measured accurately and these embryos showed the mildest phenotype. In addition, loss of Cav1 $\alpha$  results in an undulating notochord and the

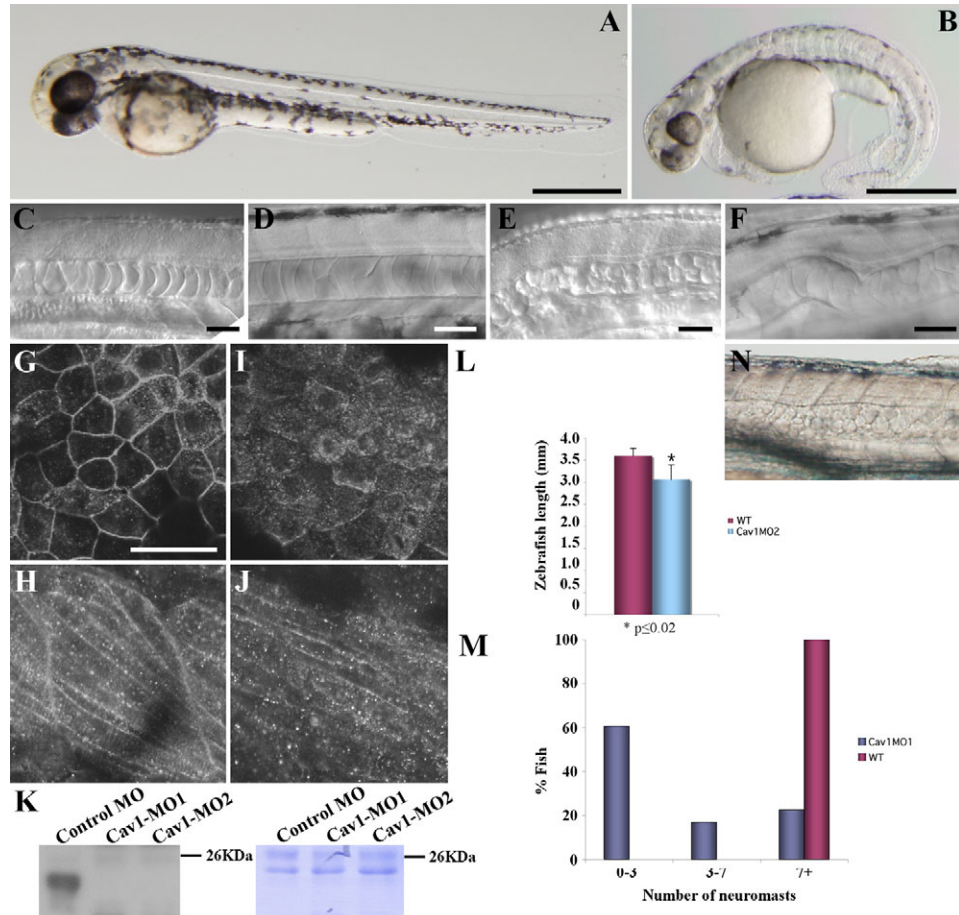


**Fig. 4.** Injection of *cav1*-MOs downregulates Cav1 expression. Embryos were injected with control MO (A,C,D,G,H) or *cav1*-MO1 (I,J) or *cav1*-MO2 (B,E,F). At 48 hours, control MO injected embryos appear normal (A), whereas embryos injected with *cav1*-MO2 are curled with disrupted notochords and tails (B). At 28 hours, control MO injected embryos have a normal notochord (C), which is also seen at 48 hours (D). In *cav1*-MO2 injected embryos the notochord appears 'bubbly' and undulating (E) and the undulating notochord is still apparent at 48 hours (F). When embryos are labelled for caveolin with the pan-caveolin antibody at 2 days post fertilisation, control MO injected embryos have normal Cav1 labelling at the cell surface (G) with normal Cav3 labelling in muscle (H), but when embryos are injected with *cav1*-MO1 at 1.5 ng/embryo, the labelling at the junction of these cells is diminished, although some weak intracellular labelling remains (I). Staining in the muscle is unaffected by *cav1*-MO1 (J compared with H). (K) Western blot analysis of *cav1*-MO1 and *cav1*-MO2 48 hours post injection labelled with the Transduction Laboratories polyclonal caveolin antibody show complete downregulation of Cav1 at 3 ng/embryo as indicated by loss of the band corresponding to caveolin (seen in the control MO lane), 10  $\mu$ g protein was loaded in each lane and Coomassie Blue staining of the membrane shows equal protein loading. (L) Injection of *cav1*-MO2 causes the body length to be reduced. The few straight embryos were measured to get fish length (*cav1*-MO2,  $n=38$ ; control MO  $n=37$ ). Error bars are standard deviation.  $P$  values were determined using two-tailed  $t$ -test for samples with equal variance. Shorter lengths are also observed in curved embryos and with *cav1*-MO1. (M) Injection of *cav1*-MO1 at 1.5 ng/embryo causes a reduced number of neuromasts at 72 hours along the posterior lateral line ( $n=71$ ) compared with control embryos. Neuromasts were identified by DASPEI labelling. (N) Loss of both Cav1 and Cav3 results in a more dramatic phenotype where small rounded cells are still evident at 48 hours. Bars, 250  $\mu$ m (A,B); 50  $\mu$ m (C-F,N); 20  $\mu$ m (G-J).

appearance of rounded vacuoles within the notochord (Fig. 4E). Ultrastructural examination of the notochord of *cav1*-MO2-injected embryos at 30 hours shows a dramatic, although somewhat variable, reduction in caveolae density within the cell-cell contact regions (40-75% decrease compared with the control MO-injected embryos from two independent experiments). This incomplete loss might reflect an overlap in function with Cav3 (Nixon et al., 2005) or Cav1 $\beta$  in the notochord, rather than incomplete knockdown of Cav1 $\alpha$ , because caveolae are undetectable in the peridermal cells of the *cav1*-MO2 injected embryos (results not shown). The notochord also shows smaller rounder vacuoles in the control

MO-injected embryos and more cellularity than the 'empty' vacuoles of the control embryos at the same stage consistent with the light microscopic observations (Fig. 5B). The medial layer of the perinotochordal basement membrane, or sheath, is also thicker and more disorganised; fibre bundles were observed at various orientations to the notochord in contrast to the uniform orientation of control MO-injected embryos (Fig. 6D). We also noted that in control MO-injected embryos the caveolae-rich plasma membranes of neighbouring cells were closely apposed (Fig. 5E). By contrast, the plasma membranes of the equivalent regions in *cav1*-MO2-injected embryos were

**Table 1. Summary of defects in zebrafish embryos observed after treatment with *cav1*-MO1 and *cav1*-MO2**

%	<i>cav1</i> -MO1 ( <i>n</i> =126)	<i>cav1</i> -MO2 ( <i>n</i> =107)	Control MO ( <i>n</i> =82)
Normal	8	6	98
Curved under	39	32	0
Notochord/tail defects	36	61	0
Severe	11	1	0
Dead	6	0	2

not closely associated and the distance between cells was variable.

In view of the incomplete loss of caveolae in the notochord, despite the inhibition of Cav1 expression as judged by western blotting (Fig. 4K), we proposed that Cav3 could contribute to caveolae formation in the notochord. This was examined by co-injection of *cav1*-MO2 and *cav3*-MO1 (Nixon et al., 2005). This caused a more severe notochord defect with round cells in the notochord still observed at 48 hours (Fig. 4N). In addition, a greater loss of morphological caveolae was observed (Fig. 5G, 84% reduction). With the unexpected localisation of both Cav1 (this study) and Cav3 (Nixon et al., 2005) in the zebrafish notochord, and in view of the functional role of Cav1 $\alpha$  in notochord development described above, we examined whether the expression of caveolin in the notochord was a feature of other vertebrates. Both mouse and chicken notochord show strong caveolin expression as judged by antibody labelling (Fig. 2F,G) consistent with an evolutionarily conserved role for caveolin in notochord function or development.

#### Loss of Cav1 $\alpha$ expression disrupts neuromast maturation

As noted above, neuromasts show strong expression of Cav1 (Fig. 1I,J,L,M and Fig. 6A,B). We investigated whether Cav1 knockdown would affect neuromast development. We used DASPEI, a vital dye, to label hair cells within the neuromasts. Injection of embryos with morpholinos targeted to *cav1* $\alpha$ , at low concentrations that result in normal embryonic morphology, causes a dramatic decrease in the number of neuromasts in the posterior lateral line at 72 hours (Fig. 4M and Fig. 6E,F). The few neuromasts that form often contain fewer hair cells than normal neuromasts at the equivalent age. The number of neuromasts in the anterior lateral line is also reduced but not to the same extent as those in the posterior lateral line. To confirm the absence of neuromasts (and not just the loss of hair cells that label with DASPEI) we performed scanning electron microscopy (SEM) of 72 hour zebrafish. Although these animals appear relatively normal, there are fewer neuromasts in embryos injected with *cav1*-MO1 at 1.5 ng/embryo (Fig. 6H,J). Quantification showed that 60% of embryos injected with *cav1*-MO1 have three or fewer neuromasts in the posterior lateral line (*n*=71) whereas 100% of WT embryos have more than seven (Fig. 4M). Only 22% of the embryos injected with *cav1*-MO1 have an equivalent number of neuromasts (7+) equivalent to control MO-injected embryos (Fig. 6D) or WT embryos (Fig. 6G,I). These studies show a vital role for Cav1 $\alpha$  in neuromast development.

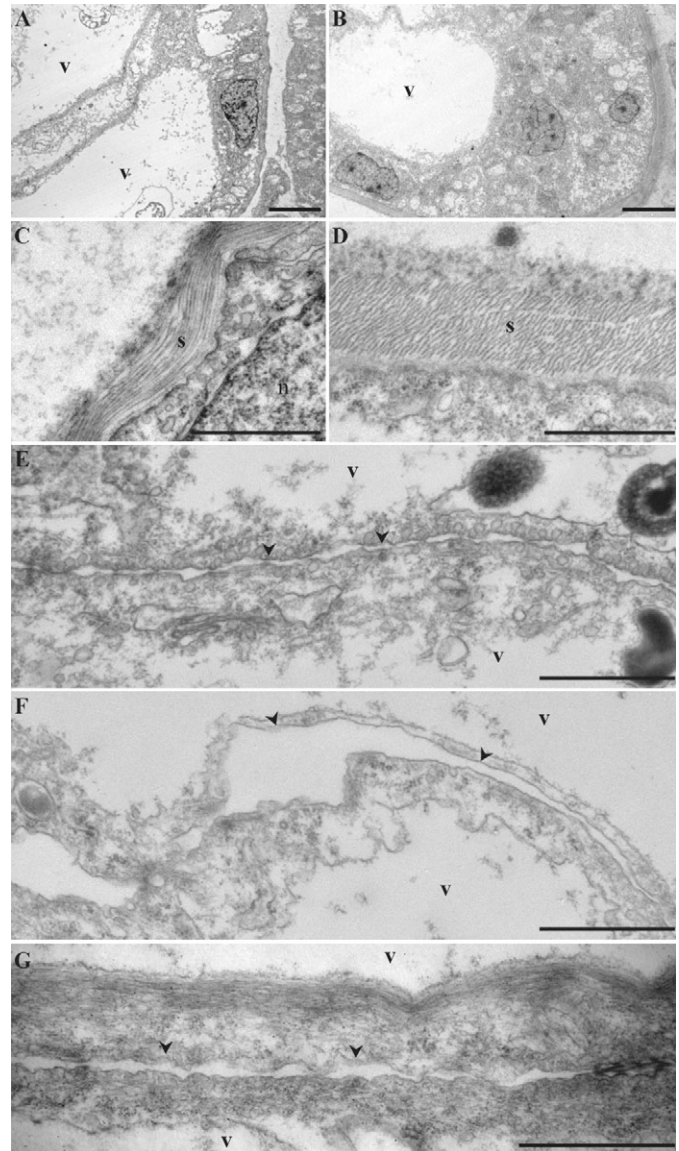


**Fig. 5.** Downregulation of *cav1* $\alpha$  disrupts normal notochord development. (A-F) Analysis of notochords in 30-hour embryos injected with control MO (A,C,E) and *cav1*-MO2 (B,D,F). Control MO injected embryos have large vacuoles and a tight undulating sheath (A,C). *cav1*-MO2 injected embryos have small vacuoles with a large amount of cellular material around the edge of the notochord (B). The sheath (s) appears to be much wider and more disorganised in *cav1*-MO2 injected embryos (D) compared with control MO injected embryos (C). *cav1*-MO2 injected embryos have many fewer caveolae and large spaces between cell membranes (F) compared with the controls (E). (G) Loss of both Cav1 and Cav3 results in a more dramatic downregulation of caveolae number. Arrowheads, membranes of individual cells; v, vacuole. Bars, 10  $\mu$ m (A,B); 1  $\mu$ m (C-G).

#### Discussion

The existence of small membrane invaginations termed caveolae has been known for over 50 years but to date their precise function is unknown. The production of knockout mice has furthered our understanding of this organelle, but it remains

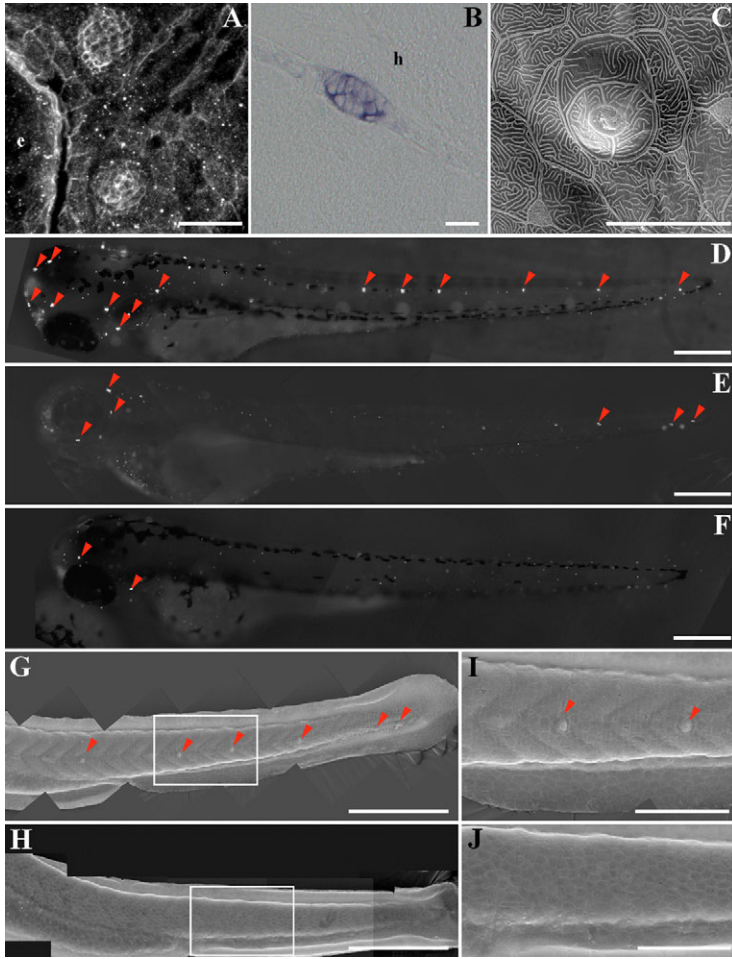


**Fig. 6.** *cav1*-MO disrupts development of neuromasts in the posterior lateral line. (A) Projected stack of confocal sections of zebrafish embryos labelled with caveolin antibody shows labelling around the neuromasts near the eye (e) at 72 hours. *Cav1* whole-mount in situ hybridisation was carried out and sections of 72-hour embryos were examined. (B) *cav1* mRNA is found throughout the neuromast. (C) Scanning electron micrograph of a 72-hour control zebrafish embryo with normal neuromasts. DASPEI labelling (D-F) and scanning electron microscopy (G-J) reveal that 72-hour control MO injected embryos have seven to eight neuromasts along their posterior lateral line (D) but when they are injected with a morpholino targeted to *cav1 $\alpha$  at 1.5 ng/embryo (*cav1*-MO1), the number of neuromasts are severely reduced (E). (F) The result was confirmed with the second morpholino to *cav1 $\alpha$  (*cav1*-MO2). (G-J) The number of neuromasts in the posterior lateral line after *cav1* MO injection was also shown to be reduced (H,J) compared with WT embryos (G,I). I and J are magnifications of the boxed areas of G and H to demonstrate the loss of neuromasts in the lateral line. h, head. Bars, 20  $\mu$ m (A-C); 250  $\mu$ m (D-H); 100  $\mu$ m (I,J).**

surprising that an organism can function without such an abundant feature of the plasma membrane. We have used the zebrafish to further our knowledge of the function of this elusive organelle. The ease of manipulating genes and the accessibility of the zebrafish embryo makes this system ideal for studying caveolin and caveolae function. We found that *Cav1* expression in signalling tissues is important for axis formation. Interestingly, we also found caveolin expressed in the notochord and neuromasts. We examined the notochord at

the ultrastructural level and discovered an incredible density of caveolae in this tissue. Consistent with the observed pattern of *Cav1* expression, we show that knockdown of this protein leads to disruption of both notochord and neuromast development.

#### *Cav1* is localised to key signalling tissues

Previous studies have examined the expression of *Cav1* in the zebrafish at limited stages. These studies localised *cav1* to the intestinal epithelium, somite borders and the heart ventricle (Smart et al., 2004) along with the notochord, neuromast, skin and vasculature (Fang et al., 2006), but did not report details of earlier *Cav1* expression. We find that *Cav1* is spatially restricted from 12 hours in the developing zebrafish embryo. As in the previous study, we find *cav1* expression in the intestine, inter-somite region and the heart but, in addition, we find expression in tissues important for developmental signalling such as the notochord (described by Fang and co-workers) and tailbud, including the Kupffer's vesicle. The notochord is an early embryonic structure that is the source of signals important for axis formation, neural differentiation and somite patterning (Adams et al., 1990; Currie and Ingham, 1996; Ericson et al., 1995; Lewis et al., 1999). The expression of *Cav1* in the notochord may reflect a role of caveolae in regulating developmental signalling events or, as we discuss later, a role for caveolae in mechanosensation. The tailbud is critical for posterior body development and contains the tail organiser regions of the zebrafish (Kanki and Ho, 1997; Melby et al., 1996). Caveolin expression in the tailbud is dynamic, with labelling evident at 16 hours, becoming more prominent by 18 hours, and then disappearing soon after 24 hours, correlating with the transient appearance of this structure. This is consistent with a role of caveolin in the regulation of signalling events at the tailbud during development.

#### Functional characterisation of *Cav1* during development

We have carefully assessed the role of *Cav1 $\alpha$  in zebrafish development using various MOs at a range of concentrations and by optimising conditions for knockdown of *Cav1 $\alpha$  protein as judged both by western blotting and by immunofluorescence. This allowed us to minimise possible toxic effects. Previous studies (Fang et al., 2006; Smart et al., 2004) showed defects in axis elongation and somite patterning, but the high levels of MO used make it difficult to rule out toxic effects. We also see these defects (including head necrosis) when we inject the *cav1 $\alpha$  MOs at high concentrations, but when used at lower concentrations and with a second non-overlapping MO to *cav1 $\alpha$  we see less-severe defects allowing us to dissect further the possible functions of caveolin and caveolae. We also designed and injected a splice-blocking MO directed to the exon2-intron2 splice junction of *cav1* which caused a reduction, but not loss, of full-length *cav1* mRNA, as judged by RT-PCR. This is consistent with contribution of maternal mRNA to caveolin expression. This MO did not cause any significant phenotype suggesting that maternal mRNA for caveolin is important at early time points.****

Our results provide new insights into Cav1 $\alpha$  function and identify novel roles for caveolin in the notochord and neuromasts of the fish.

### Cav1 is required for neuromast maturation

Neuromasts are lateral line organs that form superficial sensory organs in amphibians and fish (Dijkgraaff, 1989; Northcutt, 1992). The neuromasts are a unit of sensory hair cells with a ring of support cells surrounding them. The neuromasts detect water movements and facilitate schooling, prey capture and predator avoidance (Dijkgraaff, 1989). There are two major components of the lateral line, the anterior and posterior lateral line (including neuromasts and sensory neurons) (David et al., 2002; Metcalfe, 1985). In zebrafish, the posterior lateral line primordium begins migrating from a position posterior to the otic placode. By the end of embryogenesis, the posterior lateral line consists of seven or eight neuromasts regularly spaced along the tail (Metcalfe et al., 1985). Cav1 expression is absent from the migrating primordium but is detected in the mature neuromast from 48 hours. Expression of *cav1* appears to occur in a ring-like shape that may represent the supporting cells of the neuromast. The function of Cav1 in these cells is unknown but we have now shown that Cav1 $\alpha$  is required for their formation. Using a voltage-sensitive dye that selectively labels sensory hair cells (Harris et al., 2003), as well as scanning electron microscopy (SEM), we show that downregulation of Cav1 $\alpha$  results in reduced maturation of the neuromasts. Cav1 $\alpha$  is not required for migration of the primordium, because by 72 hours, we observe some neuromasts in the tail but not along the body of the fish. Lateral line neuromasts have striking similarities to the structure and function of the hair cells of the inner ear (Platt et al., 1989). In most mammals, it is thought that the loss of hair cells in the inner ear that results in deafness is permanent (Saunders et al., 1991; Saunders et al., 1985). However, in birds and fish, auditory hair cells are replaced by new hair cells when they are damaged (Corwin and Cotanche, 1988; Williams and Holder, 2000). A better understanding of the mechanisms involved in neuromast maturation and regeneration may therefore provide insight into triggers that may be capable of stimulating regeneration in mammalian sensory epithelia. Whether caveolae play a role in the mature neuromast is unclear from our studies, although enrichment of Cav1 in neuromasts is still apparent after 5 days of development. However, this remains an interesting possibility in view of the postulated role of caveolae in mechanosensation (Parton and Simons, 2007; Rizzo et al., 1998; Rizzo et al., 2003; Sedding et al., 2005; Yu et al., 2006).

### Cav1 in the developing notochord

The notochord is an embryonic structure in vertebrates that functions in both tissue patterning and as a supportive element. It is eventually replaced by a backbone (Stemple, 2005). In some vertebrates, such as some fish, the notochord can function as a structural element throughout the life of the animal. In zebrafish, the notochord functions as a structural element during embryogenesis and early larval development (Kimmel et al., 1995). Without a fully differentiated notochord, the embryonic axis fails to elongate correctly (Stemple et al., 1996). Consistent with the high level of Cav1 expression in the notochord, caveolae are extremely abundant, indicating an important role for these structures in notochord function and the importance of the

notochord as a powerful system to dissect caveolae function. Caveolae function in the notochord may be conserved in evolution as indicated by our observations of high levels of caveolin in the notochords of both the mouse and chicken. In addition, examination of images from an earlier ultrastructural analysis of the intervertebral joint of the teleost, *Perca flavescens* reveals abundant caveolae. This tissue is derived from the notochord and contains the sheath and highly vacuolated notochord cells (Schmitz, 1995). Extensive intermediate filament (IF) networks were also observed within these cells, and in later studies of the intervertebral joint of *Perca flavescens*, they were identified as keratins (Schmitz, 1998). Consistent with these studies, we now show the association of 10-nm-diameter filaments with the caveolae lining the regions of cell-cell contact between the notochord cells and co-staining of these regions with anti-keratin antibodies. By electron tomography, we show for the first time that these intermediate filaments appear to have an intimate connection with caveolae, and we speculate that these components may work together to keep the notochord functioning as a structural component of the embryo. In keratinocytes, keratin filaments provide mechanical integrity (Fuchs and Coulombe, 1992) and are particularly prominent in the cytoplasm of cells that are subject to mechanical stress. Normally intermediate filaments attach to sites of cell-cell adhesion, or desmosomes (Fuchs and Cleveland, 1998), but here, rather than connecting to desmosomes, we see close association with caveolae. The components involved in this link are now amenable to dissection and functional characterisation.

Downregulation of Cav1 $\alpha$  expression causes severe defects in notochord morphology. The tails of the embryo are curved, the embryo is shorter and notochord cells contain smaller vacuoles. These changes may reflect decreased internal pressure in the notochord. At the ultrastructural level, we observed a dramatic reduction in density of caveolae, a looser apposition of the plasma membranes of neighbouring cells and a change in the size of the medial layer of the sheath with the filaments apparently disorganised and less densely packed. Whether this reflects a perturbation of sheath component deposition, as observed in *sneezy*, *happy* and *dopey* mutants (loci that encode three subunits of the coatamer vesicular protein coat complex) (Coutinho et al., 2004) or a secondary effect of reduced internal pressure is as yet unclear. It is also worth noting that both Cav1 (this study) and Cav3 (Nixon et al., 2005) are expressed in the notochord of the zebrafish. This may reflect the importance of caveolae in this tissue, because both Cav1 and Cav3 can generate caveolae. In fact when we inject both MOs together we see an even greater effect on the notochord cells with the persistence of small round vacuoles and a greater loss of caveolae at 48 hours. The presence of caveolae in the strut-like interconnecting strands of closely apposed membranes in the notochord as well as their association with intermediate filaments suggest that caveolae may play a vital structural, or mechanosensory role in the notochord. When endothelial cells are subjected to fluid shear stress, the number of caveolae increases (Boyd et al., 2003; Rizzo et al., 2003). The high density of caveolae in the notochord might therefore be related to the high hydrostatic pressure in the notochord as the cells swell in response to water uptake into the glycosaminoglycan (GAG)-enriched vacuoles (Adams et al., 1990). Caveolae could also contribute a huge

area of membrane that can be released into the bulk plasma membrane when surface expansion is required. The extremely high density of caveolae in the notochord means that this mechanism could provide up to an 80% increase in plasma membrane surface area if the caveolae were to flatten out into the bulk membrane.

In conclusion, these studies reveal a vital role for caveolin in notochord and neuromast development. How caveolae contribute to these vital developmental processes can now be tested in this highly tractable experimental system.

## Materials and Methods

### Embryo collection

Zebrafish embryos were raised, removed from their chorions and fixed in 4% paraformaldehyde as described previously (Westerfield, 2000). Animals were staged according to standard criteria (Kimmel et al., 1995) or as hours post fertilisation (h). Fixed embryos were stored at  $-20^{\circ}\text{C}$  in methanol until required.

### mRNA in situ hybridisation of whole mount zebrafish embryos

In situ hybridisation was carried out as previously described (Nixon et al., 2005).

### Morpholino (MO) injection

*cav1*-MO1 antisense oligonucleotide was designed for flanking sequence to the ATG of zebrafish *cav1 $\alpha$*  with the sequence 5'-TCCCGTCTTGATCCGCT-AGTCAT-3', a second MO (*cav1*-MO2) 5'-TCATGCTGTCCCGTGCCTGAAG-TGC-3' and a standard control morpholino; control MO 5'-CCTCTTACC-TCAGTTACAATTATA-3'. The morpholinos were obtained from Gene Tools, LLC (Philomath, OR) and diluted for injection in  $1\times$  Danieau solution [58 mM NaCl, 0.7 mM KCl, 0.4 mM  $\text{MgSO}_4$ , 0.6 mM  $\text{Ca}(\text{NO}_3)_2$ , 5 mM HEPES, pH 7.6] with Phenol Red as an indicator. The *cav1 $\alpha$*  morpholinos (0.75–4.5 ng) or control MO at the same concentration was injected into fertilised zebrafish eggs between the one- and two-cell stage. To confirm that the defects we see are specific we injected either MO alone at a relatively low concentration (0.75 ng/embryo) and saw little effect, but when we injected them together we saw the same effect on the notochord as we saw with the higher concentration.

The *cav1*-MOs were co-injected with a MO to p53 (Langheinrich et al., 2002) at concentrations from 0.3–3 ng/embryo and saw no rescue of the caveolin MO phenotype. A splice-blocking MO was designed to the exon2-intron2 splice junction with the sequence 5'-AAAGTTTGTCTACCTTACCACAT-3' and injected up to 9 ng/embryo.

### Analysis of embryos

Live embryos were immobilised in embryo medium containing tricaine (0.2% 3-aminobenzoic acid ethyl ester) and examined with an Olympus SZ12 dissecting microscope, images were captured using a DP-70 camera and Olympus DP controller program. Figures were generated using Adobe Photoshop 7 or CS2; modifications were applied to whole images only except Fig. 4B where images of two different focal planes were pieced together to show the whole embryo in focus.

The total body lengths (Zebrafish lengths) were measured in mm directly with an Olympus dissecting microscope, or images of curved embryos were captured and lengths determined using the measure tool in Adobe Photoshop CS2.

### Western blot analysis of morpholino-injected embryos

Control-MO, *cav1*-MO1 or *cav1*-MO2 (3.0 ng/embryo) injected embryos at 48 hours were incubated in 100  $\mu\text{l}$  lysis buffer (150 mM NaCl, 1.0% Nonidet P-40, 0.5% deoxycholate, 0.1% SDS, 50 mM Tris-HCl, pH 8.0) on ice for 30 minutes. The embryos were sonicated at  $4^{\circ}\text{C}$  for 15 minutes, incubated on ice for an additional 30 minutes and mixed by pipetting. The lysed mix was centrifuged at 1000 rpm for 1 minute. Protein concentration was determined using the BCA assay (Pierce). 10  $\mu\text{g}$  of sample was analysed using SDS-PAGE and immunoblotted using a polyclonal Cav1 antibody from Transduction Laboratories at 1:2000. The membrane was stained for 1 minute in Coomassie Blue followed by destaining in 50% methanol to show equal protein loading.

### Antibody labelling of whole mount zebrafish embryos

Embryos were labelled as previously described (Nixon et al., 2005).

### DASPEI labelling of whole mount embryos

Live embryos were labelled with the fluorescent dye 2-[4-(dimethylamino)styryl]-N-ethylpyridinium iodide (DASPEI; Molecular Probes, Eugene, OR) as described (Balak et al., 1990; Whitfield et al., 1996). Embryos were immobilised in Tricaine and neuromasts were counted at 72 hours. All clusters of two or more cells along the posterior lateral line labelled with DASPEI were counted as neuromasts. Images were captured using an Olympus AX-70 microscope and NIH image 1.62 software.

### Electron microscopy

Embryos were fixed in 2.5% glutaraldehyde in PBS and then processed as described previously for SEM (Davies and Forge, 1987; Williams and Holder, 2000). Immunogold labelling of frozen sections was carried out on 3-day-old embryos fixed in 4% paraformaldehyde/0.1% glutaraldehyde and processed as described previously (Parton et al., 1997). Sections were labelled with a pan-cytokeratin antibody and an anti-caveolin antibody followed by labelling with PAG 15 nm for cyokeratin and anti-rabbit 10 nm gold for the caveolin according to standard techniques. Transmission electron microscopy was performed as described previously (Nixon et al., 2005). Transverse sections were prepared in the region of the distal portion of the yolk extension to compare different embryos at the same position along the rostral-caudal axis. Caveolae density was measured by examining random sections through the notochord and counting the number of surface-connected caveolae profiles per linear length of membrane (ignoring non-connected caveolae and coated pit profiles). The number of caveolae/ $\mu\text{m}^2$  was determined by taking the mean number of caveolae necks per 1  $\mu\text{m}$  length (30 hours,  $n=35$ ; 48 hours,  $n=47$ ) and multiplying by the section thickness (0.06  $\mu\text{m}$ ). This method was also used to approximate the number of caveolae/ $\mu\text{m}^2$  in mouse adipocytes and was compared with a 20  $\mu\text{m}^2$  glancing section from the same cells, where the number of caveolae were counted and 38 caveolae/ $\mu\text{m}^2$  was the result.

For electron tomography, 300 nm sections of 3-day post fertilisation embryos were stained and labelled with 15 nm gold as a fiducial marker. Dual axis tilt series from  $+60$  to  $-60$  degrees were obtained in a Tecnai F30 300 kV TEM using the SerialEM software package. Reconstruction and modelling of the data was performed using the IMOD suite of programs (Mastronarde, 1997).

### Immunofluorescence of paraffin-embedded sections

Paraffin sections were de-waxed according to standard methods. Antigens were retrieved using a modified retrieval method as follows. Samples on slides were boiled three times for 3 minutes on high in a standard microwave in 10 mM sodium citrate (pH 6.0), allowed to cool to room temperature and then treated for 2 minutes with 0.05% trypsin. For labelling sections with the cyokeratin antibody, sections were treated with proteinase K at 20  $\mu\text{g}/\text{ml}$  for 10 minutes at room temperature. Slides were then labelled according to standard protocols. Briefly, slides were incubated in 0.1% saponin for 10 minutes, quenched in 50 mM  $\text{NH}_4\text{Cl}$  for 10 minutes and blocked for 1 hour in 2% horse serum/0.2% BSA. Sections were incubated in primary antibody for 1 hour at  $37^{\circ}\text{C}$  [Pan-caveolin (Luettterforst et al., 1999), Transduction Laboratories polyclonal caveolin-1 antibody or DakoCytomation polyclonal wide spectrum cyokeratin antibody (DakoCytomation, CA)], washed four times for 5 minutes, incubated with secondary antibody at room temperature for 1 hour (anti-mouse/rabbit CY3). Samples were washed four times for 5 minutes and mounted in N-propyl gallate. Slides were imaged using an Olympus BX51 fluorescent microscope and captured using a DP-70 camera and Olympus DP controller program.

This research was supported by a Program Grant from the National Health and Medical Research Council of Australia (to R.G.P.), NIH HD22486, DC04186 and AR45575 (to M.W.) and an ARC discovery grant (to B.K.). The authors would like to thank Annika Stark and Viola Oorschot for technical assistance and Carol Wicking and Joy Richman for providing the chick and mouse sections. We also thank members of the Parton group for critical reading of the manuscript. Confocal microscopy was performed at the ACRF/IMB Dynamic Imaging Facility for Cancer Biology, established with funding from the Australian Cancer Research Foundation. The Institute for Molecular Bioscience is a Special Research Centre of the Australian Research Council.

## References

- Adams, D. S., Keller, R. and Koehl, M. A. (1990). The mechanics of notochord elongation, straightening and stiffening in the embryo of *Xenopus laevis*. *Development* **110**, 115–130.
- Balak, K. J., Corwin, J. T. and Jones, J. E. (1990). Regenerated hair cells can originate from supporting cell progeny: evidence from phototoxicity and laser ablation experiments in the lateral line system. *J. Neurosci.* **10**, 2502–2512.
- Boyd, N. L., Park, H., Yi, H., Boo, Y. C., Sorescu, G. P., Sykes, M. and Jo, H. (2003). Chronic shear induces caveolae formation and alters ERK and Akt responses in endothelial cells. *Am. J. Physiol. Heart Circ. Physiol.* **285**, H1113–H1122.
- Capozza, F., Williams, T. M., Schubert, W., McClain, S., Bouzahzah, B., Sotgia, F. and Lisanti, M. P. (2003). Absence of caveolin-1 sensitizes mouse skin to carcinogen-induced epidermal hyperplasia and tumor formation. *Am. J. Pathol.* **162**, 2029–2039.
- Cohen, A. W., Razani, B., Schubert, W., Williams, T. M., Wang, X. B., Iyengar, P., Brasaemle, D. L., Scherer, P. E. and Lisanti, M. P. (2004). Role of caveolin-1 in the modulation of lipolysis and lipid droplet formation. *Diabetes* **53**, 1261–1270.
- Cooper, M. S. and D'Amico, L. A. (1996). A cluster of noninvoluting endocytic cells at the margin of the zebrafish blastoderm marks the site of embryonic shield formation. *Dev. Biol.* **180**, 184–198.

- Corwin, J. T. and Cotanche, D. A. (1988). Regeneration of sensory hair cells after acoustic trauma. *Science* **240**, 1772-1774.
- Coutinho, P., Parsons, M. J., Thomas, K. A., Hirst, E. M., Saude, L., Campos, L., Williams, P. H. and Stemple, D. L. (2004). Differential requirements for COPI transport during vertebrate early development. *Dev. Cell* **7**, 547-558.
- Currie, P. D. and Ingham, P. W. (1996). Induction of a specific muscle cell type by a hedgehog-like protein in zebrafish. *Nature* **382**, 452-455.
- David, N. B., Sapede, D., Saint-Etienne, L., Thisse, C., Thisse, B., Dambly-Chaudiere, C., Rosa, F. M. and Ghysen, A. (2002). Molecular basis of cell migration in the fish lateral line: role of the chemokine receptor CXCR4 and of its ligand, SDF1. *Proc. Natl. Acad. Sci. USA* **99**, 16297-16302.
- Davies, S. and Forge, A. (1987). Preparation of the mammalian organ of Corti for scanning electron microscopy. *J. Microsc.* **147**, 89-101.
- Dijkgraaf, S. (1989). The mechanosensory lateral line. In *Neurobiology and Evolution* (ed. S. Coombs, P. Gorner and H. Munz), pp. 7-14. New York: Springer.
- Drab, M., Verkade, P., Elger, M., Kasper, M., Lohn, M., Lauterbach, B., Menne, J., Lindschau, C., Mende, F., Luft, F. C. et al. (2001). Loss of caveolae, vascular dysfunction, and pulmonary defects in caveolin-1 gene-disrupted mice. *Science* **293**, 2449-2452.
- Ericson, J., Muhr, J., Placzek, M., Lints, T., Jessell, T. M. and Edlund, T. (1995). Sonic hedgehog induces the differentiation of ventral forebrain neurons: a common signal for ventral patterning within the neural tube. *Cell* **81**, 747-756.
- Fang, P. K., Solomon, K. R., Zhuang, L., Qi, M., McKee, M., Freeman, M. R. and Yelick, P. C. (2006). Caveolin-1 $\alpha$  and -1 $\beta$  perform nonredundant roles in early vertebrate development. *Am. J. Pathol.* **169**, 2209-2222.
- Fernandez, M. A., Albor, C., Ingelmo-Torres, M., Nixon, S. J., Ferguson, C., Kurzchalia, T., Tebar, F., Enrich, C., Parton, R. G. and Pol, A. (2006). Caveolin-1 is essential for liver regeneration. *Science* **313**, 1628-1632.
- Fra, A. M., Williamson, E., Simons, K. and Parton, R. G. (1995). De novo formation of caveolae in lymphocytes by expression of VIP21-caveolin. *Proc. Natl. Acad. Sci. USA* **92**, 8655-8659.
- Frank, P. G., Galbiati, F., Volonte, D., Razani, B., Cohen, D. E., Marcel, Y. L. and Lisanti, M. P. (2001). Influence of caveolin-1 on cellular cholesterol efflux mediated by high-density lipoproteins. *Am. J. Physiol. Cell Physiol.* **280**, C1204-C1214.
- Fuchs, E. and Coulombe, P. A. (1992). Of mice and men: genetic skin diseases of keratin. *Cell* **69**, 899-902.
- Fuchs, E. and Cleveland, D. W. (1998). A structural scaffolding of intermediate filaments in health and disease. *Science* **279**, 514-519.
- Gompel, N., Cubedo, N., Thisse, C., Thisse, B., Dambly-Chaudiere, C. and Ghysen, A. (2001). Pattern formation in the lateral line of zebrafish. *Mech. Dev.* **105**, 69-77.
- Harris, J. A., Cheng, A. G., Cunningham, L. L., MacDonald, G., Raible, D. W. and Rubel, E. W. (2003). Neomycin-induced hair cell death and rapid regeneration in the lateral line of zebrafish (*Danio rerio*). *J. Assoc. Res. Otolaryngol.* **4**, 219-234.
- Kanki, J. P. and Ho, R. K. (1997). The development of the posterior body in zebrafish. *Development* **124**, 881-893.
- Kimmel, C. B., Ballard, W. W., Kimmel, S. R., Ullmann, B. and Schilling, T. F. (1995). Stages of embryonic development of the zebrafish. *Dev. Dyn.* **203**, 253-310.
- Kogo, H. and Fujimoto, T. (2000). Caveolin-1 isoforms are encoded by distinct mRNAs. Identification of mouse caveolin-1 mRNA variants caused by alternative transcription initiation and splicing. *FEBS Lett.* **465**, 119-123.
- Langheirich, U., Hennen, E., Stott, G. and Vacun, G. (2002). Zebrafish as a model organism for the identification and characterization of drugs and genes affecting p53 signaling. *Curr. Biol.* **12**, 2023-2028.
- Le Lay, S., Krief, S., Farnier, C., Lefrere, I., Le Liepvre, X., Bazin, R., Ferre, P. and Dugail, I. (2001). Cholesterol, a cell size-dependent signal that regulates glucose metabolism and gene expression in adipocytes. *J. Biol. Chem.* **276**, 16904-16910.
- Lewis, K. E., Currie, P. D., Roy, S., Schauerte, H., Haffter, P. and Ingham, P. W. (1999). Control of muscle cell-type specification in the zebrafish embryo by Hedgehog signalling. *Dev. Biol.* **216**, 469-480.
- Li, T., Sotgia, F., Vuolo, M. A., Li, M., Yang, W. C., Pestell, R. G., Sparano, J. A. and Lisanti, M. P. (2006). Caveolin-1 mutations in human breast cancer: functional association with estrogen receptor alpha-positive status. *Am. J. Pathol.* **168**, 1998-2013.
- Luetterforst, R., Stang, E., Zorzi, N., Carozzi, A., Way, M. and Parton, R. G. (1999). Molecular characterization of caveolin association with the Golgi complex: identification of a cis-Golgi targeting domain in the caveolin molecule. *J. Cell Biol.* **145**, 1443-1459.
- Mastroratte, D. N. (1997). Dual-axis tomography: an approach with alignment methods that preserve resolution. *J. Struct. Biol.* **120**, 343-352.
- Melby, A. E., Warga, R. M. and Kimmel, C. B. (1996). Specification of cell fates at the dorsal margin of the zebrafish gastrula. *Development* **122**, 2225-2237.
- Metcalfe, W. K. (1985). Sensory neuron growth cones comigrate with posterior lateral line primordial cells in zebrafish. *J. Comp. Neurol.* **238**, 218-224.
- Metcalfe, W. K., Kimmel, C. B. and Schabtach, E. (1985). Anatomy of the posterior lateral line system in young larvae of the zebrafish. *J. Comp. Neurol.* **233**, 377-389.
- Murata, M., Peranen, J., Schreiner, R., Wieland, F., Kurzchalia, T. V. and Simons, K. (1995). VIP21/caveolin is a cholesterol-binding protein. *Proc. Natl. Acad. Sci. USA* **92**, 10339-10343.
- Nixon, S. J., Wegner, J., Ferguson, C., Mery, P. F., Hancock, J. F., Currie, P. D., Key, B., Westerfield, M. and Parton, R. G. (2005). Zebrafish as a model for caveolin-associated muscle disease: caveolin-3 is required for myofibril organization and muscle cell patterning. *Hum. Mol. Genet.* **14**, 1727-1743.
- Northcutt, R. G. (1992). Distribution and innervation of lateral line organs in the axolotl. *J. Comp. Neurol.* **325**, 95-123.
- Parton, R. G. (2001). Cell biology. Life without caveolae. *Science* **293**, 2404-2405.
- Parton, R. G. and Simons, K. (2007). The multiple faces of caveolae. *Nat. Rev. Mol. Cell Biol.* **8**, 185-194.
- Parton, R. G., Way, M., Zorzi, N. and Stang, E. (1997). Caveolin-3 associates with developing T-tubules during muscle differentiation. *J. Cell Biol.* **136**, 137-154.
- Platt, C., Popper, A. N. and Fay, R. R. (1989). The ear as part of the octavolateralis system. In *The Mechanosensory Lateral Line: Neurobiology and Evolution* (ed. S. Coombs, P. Gorner and H. Munz), pp. 633-651. New York: Springer-Verlag.
- Radel, C. and Rizzo, V. (2005). Integrin mechanotransduction stimulates caveolin-1 phosphorylation and recruitment of Csk to mediate actin reorganization. *Am. J. Physiol. Heart Circ. Physiol.* **288**, H936-H945.
- Razani, B. and Lisanti, M. P. (2001). Caveolin-deficient mice: insights into caveolar function human disease. *J. Clin. Invest.* **108**, 1553-1561.
- Razani, B., Engelman, J. A., Wang, X. B., Schubert, W., Zhang, X. L., Marks, C. B., Macaluso, F., Russell, R. G., Li, M., Pestell, R. G. et al. (2001). Caveolin-1 null mice are viable but show evidence of hyperproliferative and vascular abnormalities. *J. Biol. Chem.* **276**, 38121-38138.
- Razani, B., Combs, T. P., Wang, X. B., Frank, P. G., Park, D. S., Russell, R. G., Li, M., Tang, B., Jelicks, L. A., Scherer, P. E. et al. (2002). Caveolin-1-deficient mice are lean, resistant to diet-induced obesity, and show hypertriglyceridemia with adipocyte abnormalities. *J. Biol. Chem.* **277**, 8635-8647.
- Rizzo, V., McIntosh, D. P., Oh, P. and Schnitzer, J. E. (1998). In situ flow activates endothelial nitric oxide synthase in luminal caveolae of endothelium with rapid caveolin dissociation and calmodulin association. *J. Biol. Chem.* **273**, 34724-34729.
- Rizzo, V., Morton, C., DePaola, N., Schnitzer, J. E. and Davies, P. F. (2003). Recruitment of endothelial caveolae into mechanotransduction pathways by flow conditioning in vitro. *Am. J. Physiol. Heart Circ. Physiol.* **285**, H1720-H1729.
- Rothberg, K. G., Heuser, J. E., Donzell, W. C., Ying, Y. S., Glenney, J. R. and Anderson, R. G. (1992). Caveolin, a protein component of caveolae membrane coats. *Cell* **68**, 673-682.
- Sato, K., Sato, M., Audhya, A., Oegema, K., Schweinsberg, P. and Grant, B. D. (2006). Dynamic regulation of caveolin-1 trafficking in the germ line and embryo of *Caenorhabditis elegans*. *Mol. Biol. Cell* **17**, 3085-3094.
- Saunders, J. C., Dear, S. P. and Schneider, M. E. (1985). The anatomical consequences of acoustic injury: a review and tutorial. *J. Acoust. Soc. Am.* **78**, 833-860.
- Saunders, J. C., Cohen, Y. E. and Szymko, Y. M. (1991). The structural and functional consequences of acoustic injury in the cochlea and peripheral auditory system: a five year update. *J. Acoust. Soc. Am.* **90**, 136-146.
- Scheel, J., Srinivasan, J., Honnert, U., Henske, A. and Kurzchalia, T. V. (1999). Involvement of caveolin-1 in meiotic cell-cycle progression in *Caenorhabditis elegans*. *Nat. Cell Biol.* **1**, 127-129.
- Scherer, P. E., Okamoto, T., Chun, M., Nishimoto, I., Lodish, H. F. and Lisanti, M. P. (1996). Identification, sequence, and expression of caveolin-2 defines a caveolin gene family. *Proc. Natl. Acad. Sci. USA* **93**, 131-135.
- Schmitz, R. J. (1995). Ultrastructure and function of cellular components of the intercentral joint in the percoid vertebral column. *J. Morphol.* **226**, 1-24.
- Schmitz, R. J. (1998). Immunohistochemical identification of the cytoskeletal elements in the notochord cells of bony fishes. *J. Morphol.* **236**, 105-116.
- Sedding, D. G., Hermesen, J., Seay, U., Eickelberg, O., Kummer, W., Schwenke, C., Strasser, R. H., Tillmanns, H. and Braun-Dullaues, R. C. (2005). Caveolin-1 facilitates mechanosensitive protein kinase B (Akt) signaling in vitro and in vivo. *Circ. Res.* **96**, 635-642.
- Smart, E. J., De Rose, R. A. and Farber, S. A. (2004). Annexin 2-caveolin 1 complex is a target of ezetimibe and regulates intestinal cholesterol transport. *Proc. Natl. Acad. Sci. USA* **101**, 3450-3455.
- Stemple, D. L. (2005). Structure and function of the notochord: an essential organ for chordate development. *Development* **132**, 2503-2512.
- Stemple, D. L., Solnica-Krezel, L., Zwartkruis, F., Neuhauss, S. C., Schier, A. F., Malicki, J., Stainier, D. Y., Abdelilah, S., Rangini, Z., Mountcastle-Shah, E. et al. (1996). Mutations affecting development of the notochord in zebrafish. *Development* **123**, 117-128.
- Tang, Z., Scherer, P. E., Song, K., Chu, C., Kohtz, D. S., Nishimoto, I., Lodish, H. F. and Lisanti, M. P. (1996). Molecular cloning of caveolin-3, a novel member of the caveolin gene family expressed predominantly in muscle. *J. Biol. Chem.* **271**, 2255-2261.
- Tang, Z., Okamoto, T., Boontrakulpoontawe, P., Katada, T., Otsuka, A. J. and Lisanti, M. P. (1997). Identification, sequence, and expression of an invertebrate caveolin gene family from the nematode *Caenorhabditis elegans*. Implications for the molecular evolution of mammalian caveolin genes. *J. Biol. Chem.* **272**, 2437-2445.
- Trigatti, B. L., Anderson, R. G. and Gerber, G. E. (1999). Identification of caveolin-1 as a fatty acid binding protein. *Biochem. Biophys. Res. Commun.* **255**, 34-39.
- Way, M. and Parton, R. G. (1995). M-caveolin, a muscle-specific caveolin-related protein. *FEBS Lett.* **376**, 108-112.
- Westerfield, M. (2000). *The Zebrafish Book. A Guide for the Laboratory Use of Zebrafish (Danio rerio)*. Eugene: University of Oregon Press.
- Whitfield, T. T., Granato, M., van Eeden, F. J., Schach, U., Brand, M., Furutani-Seiki, M., Haffter, P., Hammerschmidt, M., Heisenberg, C. P., Jiang, Y. J. et al. (1996). Mutations affecting development of the zebrafish inner ear and lateral line. *Development* **123**, 241-254.
- Williams, J. A. and Holder, N. (2000). Cell turnover in neuromasts of zebrafish larvae. *Hear. Res.* **143**, 171-181.
- Williams, T. M. and Lisanti, M. P. (2005). Caveolin-1 in oncogenic transformation, cancer, and metastasis. *Am. J. Physiol. Cell Physiol.* **288**, C494-C506.